Ⅲ. 研究成果の刊行物・別刷

Dynamic Activity Dependence of In Vivo Normal Knee Kinematics

Taka-aki Moro-oka,[1,2] Satoshi Hamai,[2] Hiromasa Miura,[2] Takeshi Shimoto,[3] Hidehiko Higaki,[3] Benjamin J. Fregly,[1] Yukihide Iwamoto,[2] Scott A. Banks[1,4]

[1]Department of Mechanical and Aerospace Engineering, University of Florida, 318 MAE-A, Mail Stop 116250, Gainesville, Florida 32611

[2]Department of Orthopaedic Surgery, Graduate School of Medical Sciences, Kyushu University, Fukuoka, Japan

[3]Department of Mechanical Engineering, Faculty of Engineering, Kyushu Sangyo University, Fukuoka, Japan

[4]The BioMotion Foundation, Palm Beach, Florida

Received 20 November 2006; accepted 25 January 2007

Published online in Wiley InterScience (www.interscience.wiley.com). DOI 10.1002/jor.20488

ABSTRACT: Dynamic knee kinematics were analyzed for normal knees in three activities, including two different types of maximum knee flexion. Continuous X-ray images of kneel, squat, and stair climb motions were taken using a large flat panel detector. CT-derived bone models were used for model registration-based 3D kinematic measurement. Three-dimensional joint kinematics and contact locations were determined using three methods: bone-fixed coordinate systems, interrogation of CT-based bone model surfaces, and interrogation of MR-based articular cartilage model surfaces. The femur exhibited gradual external rotation throughout the flexion range. Tibiofemoral contact exhibited external rotation, with contact locations translating posterior while maintaining 15° to 20° external rotation from 20° to 80° of flexion. From 80° to maximum flexion, contact locations showed a medial pivot pattern. Kinematics based on bone-fixed coordinate systems differed from kinematics based on interrogation of CT and MR surfaces. Knee kinematics varied significantly by activity, especially in deep flexion. No posterior subluxation occurred for either femoral condyle in maximum knee flexion. Normal knees accommodate a range of motions during various activities while maintaining geometric joint congruency. © 2007 Orthopaedic Research Society. Published by Wiley Periodicals, Inc. J Orthop Res 26:428–434, 2008

Keywords: tibiofemoral joint; kinematics; dynamic activity; flat panel detector; 3D/2D model registration; tibiofemoral contact

INTRODUCTION

3D-to-2D model registration techniques have been used to measure normal in vivo knee kinematics from radiographic images. These studies have provided clinically insightful information and spurred further complementary investigations. Research topics of current interest include exploration of knee kinematics over the full flexion range and development of techniques for generating and reporting data to provide enhanced physiologic insight.

3D kinematics studies have focused on motion from 0° to 90° of flexion. Asano et al.[1] reported a medial pivot motion pattern during static weight bearing from 0° to 90°. Komistek et al.[2] reported dynamic normal knee kinematics using shape-matching techniques with computed tomography (CT)-derived bone models. They showed that the lateral condyle experienced significantly more AP translation in activities up to 90° of flexion with no significant differences among activities. More recently, Li et al.[3] reported cartilage contact kinematics from 0° to 90° using bi-plane fluoroscopy and MRI-derived bone models. No study has analyzed dynamic, weight-bearing tibiofemoral motion from extension to maximum knee flexion.

3D knee kinematic studies also have used a variety of coordinate systems and joint contact computations to describe findings, making it sometimes difficult to compare results of one study to another. For example, varus–valgus motion determined from coordinate systems embedded in the bones can be interpreted to indicate separation of the joint surfaces. However, when the different sagittal slopes of the medial and lateral tibial surfaces are considered, varus–valgus motion can result from the condyles moving AP while remaining in contact with these surfaces. A complete

Correspondence to: Scott A. Banks (Telephone: 352-392-6109; Fax: 352-392-7303; E-mail: banks@ufl.edu)

mapping of joint surface separations provides a coordinate system-independent measure of articular apposition that avoids misinterpretation. To date, CT-derived bone models (CT model) have been primarily used for model registration-based kinematic measurements.[1,2,4] Determination of tibiofemoral contact conditions from CT models assumes uniform cartilage thickness. MR-based surface models including cartilage are superior for computing surface interactions, but suffer from less accurate bone definition, which can lead to less precise kinematic measurements.[5] The optimal approach, therefore, might be to perform model registration using CT-derived bone models with surface interrogations performed using MR-derived articular surfaces.

The purpose of this study was to analyze healthy knee kinematics in three activities from extension to maximum knee flexion using high-resolution dynamic flat-panel detector images. A secondary purpose was to consider cartilage thickness in tibiofemoral contact analysis and to compare different methods for reporting articular kinematics.

MATERIALS AND METHODS

Six healthy male subjects, averaging 29 years (28–31), 171 cm (165–177), and 69 kg (55–80) gave informed consent to participate in this study as approved by the institutional review board. Bone models of the femur and tibia/fibula were created from CT (Toshiba, Aquilion, Tochigi, Japan) and MR (Hitachi, Airis II Comfort, Tokyo) scans of one leg. CT scans used a 512 × 512 image matrix, a 0.35 × 0.35 pixel dim, and a 1-mm thickness spanning approximately 150 mm above and below the joint line of the knee, and 2 mm slices through the centers of the hip and ankle. MR scans used a 512 × 512 image matrix, a 0.39 × 0.39 pixel dim, and a 1-mm thickness spanning more than 80 mm above and below the joint line of the knee. Scan time of MR ranged from 11 to 15 min. Exterior cortical bone edges for CT and external edges of both cortical bone and cartilage for MRI were segmented using commercial software (SliceOmatic, Tomovision, Montreal, CA), and these point clouds were converted into polygonal surface models (Geomagic Studio, Raindrop Geomagic, Research Triangle Park, NC). Anatomic coordinate systems were embedded in each bone model following conventions of previous studies.[5] The coordinate systems were first defined for the CT models. The mediolateral (Z) axis of both the femur and tibia/fibula was defined by fitting a cylinder to each posterior condyle of the femur (Fig. 1). The mid point of the cylindrical axis was defined as the coordinate system origin. The proximal/distal (Y) axis for the femur was defined by a line perpendicular to the cylindrical axis in the plane intersecting the femoral head center. The proximal/distal (Y) axis for the shank

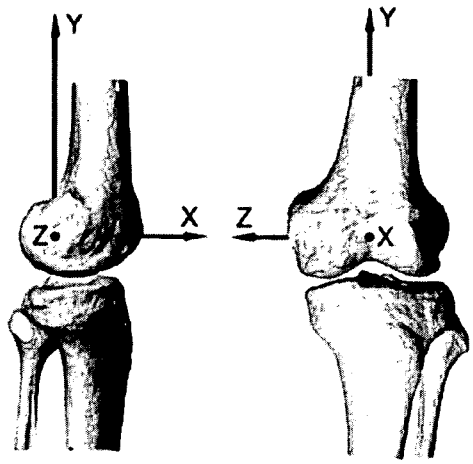

Figure 1. The mediolateral (2) axis of both the femur and tibia/fibula was defined by fitting a cylinder to the posterior condyles of the femur. The mid point of the cylindrical axis was defined as the coordinate system origin for both tibin and femur.

was perpendicular to the cylindrical axis in the plane intersecting the ankle center. The anteroposterior (X) axis was formed from the cross product of the first two. Next, the MR model was registered with the corresponding CT model in its initial reference pose in order to align the embedded coordinate systems in each bone model. Proprietary automated alignment software was used to match 3D bone surfaces (Geomagic Studio). Reported accuracy for this technique is less than 0.1 micrometers in length and 0.1 arcseconds in angle compared to a reference standard value.

Continuous sagittal X-ray images of kneel, squat, and stair-climb activities for each subject were taken using a flat panel detector (Hitachi, Clavis, 3 frames/s, image area 397 × 298 mm, 0.20 × 0.20 mm/pixel resolution) (Fig. 2). For the kneel activity, subjects placed their leg on a box, with the foot and ankle hanging freely, and applied their body weight to achieve maximum knee flexion. For the squat activity, the subject stood on a wheeled cart, moved rearward at >2.5 cm/s, so their knee position could be maintained in front of the flat-panel detector as they flexed from full extension to full flexion. For the stair activity, subjects ascended a two-step staircase in a reciprocal manner with knee motions recorded on the first step. A total of 293 images were used: 90 images for kneel, 130 for squat, and 73 for stair.

The 3D position and orientation of the tibia/fibula and femur were determined using previously reported shape matching techniques[4–6] (Fig. 3). A region of the flat-panel X-ray image was extracted and scaled to 512 × 512 square pixels for 3D shape registration. The CT models were projected onto the X-ray image and manually aligned with the bone projections. An automated matching algorithm using nonlinear least squares optimization, and an image edge-to-model edge distance criteria was used to refine registration of the bone models. RMS errors for this method were 0.53 mm for in-plane

Figure 2. Subjects performed kneeling (left), lunge (middle) and stair (right) activities while their knee motion was observed using a large flat panel x-ray image detector. The images show a left knee being studied. Kneeling was performed from 90° to maximum comfortable flexion. Squatting was performed from a standing position to maximum comfortable flexion. The stair activity captured the ascent phase from approximately 70° to 10° flexion.

translation, 1.6 mm for out-of-plane translation, and 0.54° for rotations in a previous study.[5] Propagation of these uncertainties to the articular surfaces results in a 95% confidence interval >2 mm for declaring separation of the femoral condyles from the tibial surface.

The kinematics of the joint were determined from the 3D position of each bone model using Cardan angles as described by Tupling and Pierrynowski.[7] Knee rotations were analyzed as a function of flexion angle. Spline interpolation with 5° flexion increments was used to create average kinematics for the group. The stair climb proceeded from flexion to extension; the kneel and squat proceeded from extension to flexion. Each subject began and completed each activity at slightly different flexion angles, so averages are reported for flexion angles from three to six knees. One-way ANOVA and post hoc tests (Bonferroni/Dunn) ($p < 0.05$) were used to examine differences among overall results.

The surface of each CT-derived tibial model was divided into medial and lateral compartments and represented as a cloud of points. For every image, a surface separation map was created by computing the minimum distance between each point on the tibial surface and all points on the femoral surface (Fig. 4). Medial and lateral condylar contact locations were computed as the geometric centroid of the region having <6 mm separation, which acknowledges uncertainty about cartilage thickness,[8,9] cartilage deformation, and measurement errors. The choice of separation threshold had a negligible effect on centroid location for thresholds above 3 mm. The angle between the kinematics of the femur with respect to the tibia.

Interactions of cartilage surfaces were determined from the MR-derived models. The bony part of the MR models was registered with the corresponding CT models using automated alignment software (Geomagic Studio). Knee kinematics determined from CT model registration were then used to orient the cartilage surfaces. Contact points were defined in the same manner for the MR models, except a 2-mm maximum separation threshold was used to define the region of contact, contact centroids, and rotational kinematics (Fig. 4).

RESULTS

Bony kinematics varied among activities. Femoral rotation during squatting was significantly different from kneeling at all flexion angles and differed from stair climbing from 25° to 35° flexion (Fig. 5A). However, the femur rotated externally with flexion in all three activities. Sharp external rotation was seen from 0° to 15° in squatting,

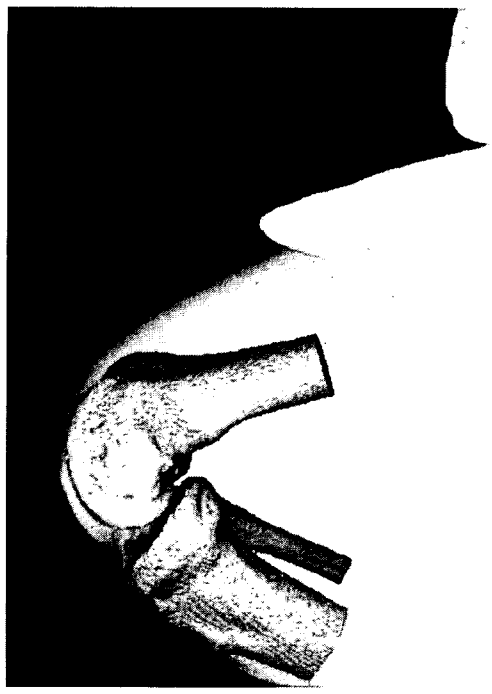

Figure 3. 3D-to-2D CT model-to-flat panel image registration was used to determine the kinematics of healthy knees during three weight bearing activities.

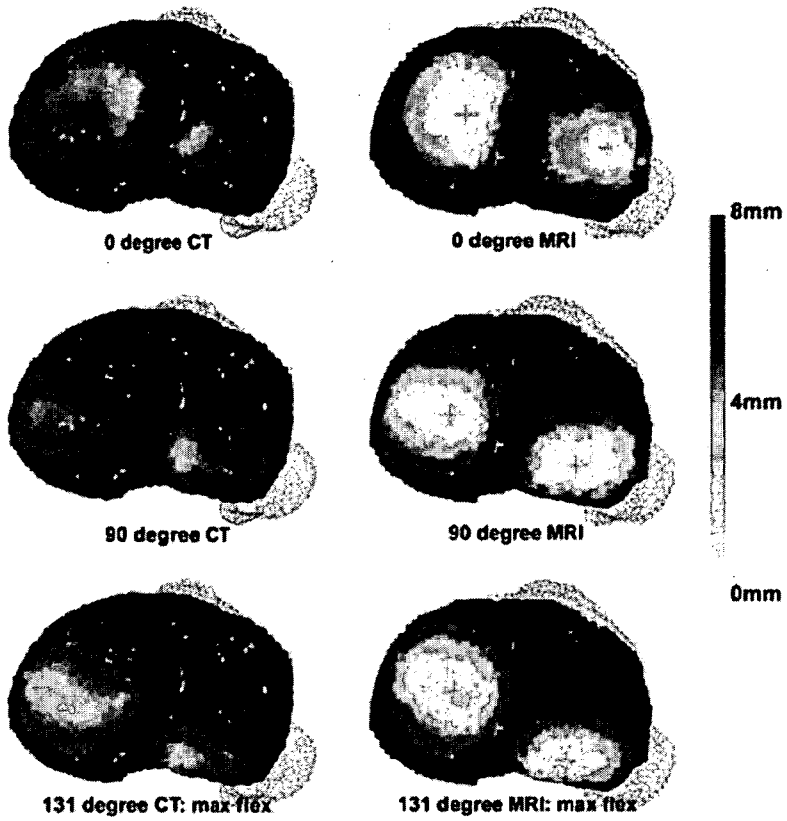

Figure 4. Separation distance mapping for squat at 0°, 90°, and maximum flexion (131°) in one subject. Pictures calculated from the MRI model and CT model are shown at the same flexion angle. The centroids of the contact areas are shown as a red cross to indicate the estimated contact location. The picture shows irregular estimated contact regions based on the CT derived models, while the MR derived models of articular cartilage show uniformly rounded contact region estimates

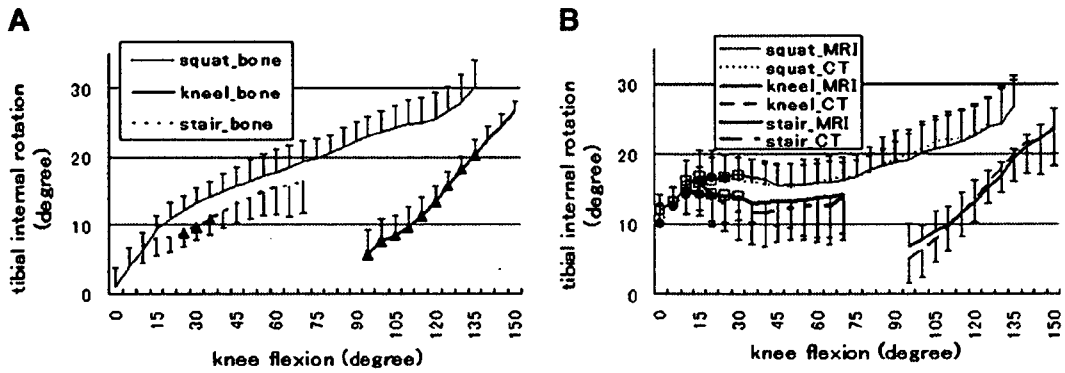

Figure 5. Femoral external rotation increased with knee flexion for stair, squat and kneel activities. A: Femoral external rotations based on bone-embedded coordinate systems. Solid triangles on the stair and kneel represent statistically significant differences from the corresponding rotation during the squat activity ($p < 0.05$). B: Femoral external rotations based on contact locations determined from MR and CT derived cartilage and bone models, respectively. There were no statistically significant differences between rotations measured by these two methods. Solid squares represent significant differences between rotations determined by the MR model based contact locations and the regid body bone motions in graph A ($p < 0.05$). Solid circles represent significant differences between rotations determined by the CT model based contact locations and the rigid body bone motions in graph A ($p < 0.05$).

similar to the "screw home" movement reported for passive knee motions.[10]

The regions used to estimate contact location were irregularly shaped for the CT models and consistently circular or elliptical for the MR models (Fig. 4). Rotations determined from the CT and MR model contact points were not significantly different (Figs. 4 and 5B). There were significant differences between rotations determined from rigid body bone kinematics and contact points for stair and squat activities at flexion angles <30° (Fig. 5A and B). There were no statistically significant differences between rotations measured by MR derived model and CT derived model.

AP translation of the condylar contact regions showed three phases over the range of motion (Fig. 6). From extension to 20° flexion, the contact points rotated externally with posterior translation. From 20° to 80°, they translated posteriorly with little additional rotation. For flexion >80° (squat and kneel), additional external rotation resulted predominantly from posterior lateral translation, essentially pivoting about the medial compartment. There were significant differences in lateral contact positions between squat and kneel from 100°–139° flexion (<0.01 for 100° to 135°, and $p=0.015$ at 139°). There were no differences in contact positions for the medial condyle.

Condylar separation was not observed at flexion <150°. In two subjects the minimum medial surface separation exceeded 2 mm (MR cartilage model) in terminal kneeling at >150° flexion.

DISCUSSION

This study examined dynamic 3D normal knee kinematics in three activities, including two types of maximum knee flexion, using a high-resolution flat panel X-ray detector. Different values of knee axial rotation were observed with different activities, with the greatest femoral external rotation observed during the squat activity. No subluxation of the lateral femoral condyle was observed in maximum knee flexion, and condylar separation from the tibial surface was not commonly observed. Rigid body kinematics measured from bone-embedded coordinate systems produced different joint axial rotations than were measured from the orientation of the medial and lateral condylar contact locations for flexion <30°.

Knee axial rotations differed according to the method of calculation. Rotations defined from bone-embedded coordinate systems showed gradual femoral external rotation across the entire flexion arc (Fig. 5A). Rotations measured from condylar

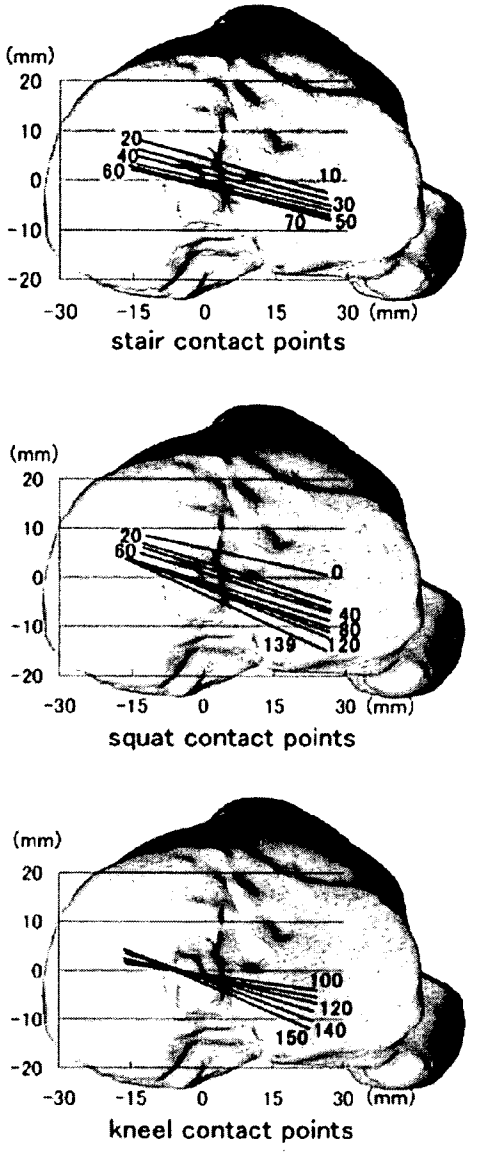

Figure 6. Average contact locations superimposed on an MR model of the tibial surface. For all activities, the contact points in the lateral compartment moved from anterior to posterior with knee flexion. Contact locations are shown for 10° flexion increments for stair and kneel activities, 20° flexion increments for the squat activity. There were no significant differences between contact locations for the squat and stair activites.

contact locations exhibited three phases: sharp external rotation from 0° to 15° flexion, relatively constant rotation from 20° to 80° flexion, and increasing rotation from 80° to 150° flexion (Fig. 5B). Significant differences in early flexion (0° to 30°) are due to femoral geometry. Iwaki et al.[11] showed that the sagittal profile of the medial femoral condyle is composed of a larger distal and smaller posterior circular arc, while the lateral condyle is well described by a single circular facet.

From extension to mid flexion, the medial tibial contact area had a more ovoid shape and moved posteriorly (Figs. 5 and 6). This relative internal rotation of the contact locations was offset by relative external femoral rotation, resulting in less rotation measured at the contact locations than was measured from the bone-embedded coordinate systems over this range. From 20° to 80° flexion the contact locations moved posterior, inclined 15° to 20° with respect to the tibia, maintaining the femur approximately in line with the foot as previously reported.[11] However, unlike previous reports, contact-derived rotation continued from 80° to full flexion in squat and kneel. From 80° to maximum flexion, the contact-derived and rigid body bone rotations showed similar curves, which is reasonable considering the circular geometry of the posterior femoral condyles.[11]

Banks et al.[12] showed kinematics varied with implant design and activity in total knee arthroplasty patients. In this study, kinematics varied with activity in healthy knees, particularly with squat and kneel. The greatest total rotation and the most posterior lateral contact was observed with squatting, but the maximum flexion angle and the rate of tibial rotation from 100° to maximum flexion was greater with kneeling. Medial contact was in the same area for both activities. The lateral femoral condyle translated to the posterior edge of the tibial surface during squat, although there was no subluxation. Subjects were encouraged to achieve comfortable maximum flexion, thus results may have differed if the squat was forced to greater knee flexion.

Comparison of stair climb and squat activities revealed small kinematic differences in the middle range of flexion, which were not statistically significant. The femur showed greater external rotation for all flexion angles during squatting. Results from cadaver studies,[11] MRIs of living knees,[13] and living knees with RSA[14] have shown that a posture with tibial external rotation can suppress tibial internal rotation over the flexion arc. The wider stance width used during the squat activity probably biased the knee toward greater femoral external rotation in the mid range of flexion. Standard deviations for the squat and stair activities were 20% greater than for the kneel activity, suggesting kneeling is more geometrically constrained or stereotypic.

Surface distance calculations revealed only two cases showing evidence of condylar separation, both occurring at terminal flexion in kneeling beyond 150°. In the static MRI study of maximally flexed knees, Nakagawa et al.[15] reported the medial condyle remained positioned over the tibial articular surface but lifted away from it, mechanistically similar to the present finding. Two differences may account for infrequent observation of condylar separation in this study. First, a conservative threshold (95% confidence interval) was used for declaring separation, acknowledging uncertainty accrued from measurement uncertainty, surface modeling errors, and possible cartilage deformation. Second, Nakagawa et al.[15] studied a different activity. In this study, subjects knelt to maximum passive flexion with partial body weight and an upright trunk posture (hip angle approximately 90°). The subjects reported in Nakagawa et al.[15] were supine, with the hip extended in the MRI scanner, similar to an athlete's quadriceps stretching posture. Hip extension might have caused greater quadriceps tension and resulted in a more exaggerated joint posture.

Nakagawa et al.[15] also concluded that the lateral femoral condyle subluxed posteriorly from the tibia at full passive flexion, a phenomenon not seen in the present study. Nakagawa et al.[15] tracked a cylindrical axis embedded in the posterior condyles and determined that subluxation occurred when the lateral axis moved posterior to the tibial surface at 162° flexion. However, subluxation is an articular phenomenon where the surfaces of a joint no longer face each other exactly but remain partially aligned. MR and cryosection pictures in the report of Nakagawa et al.[15] show the lateral femoral condyle has adequate contact with the edge of the tibial articular surface even when the cylindrical axis has exceeded the tibial periphery. These pictures are consistent with the observations of this study.

Findings of articular separation and subluxation in healthy joints sometimes can result from methodological issues and sometimes from articular reality. In the latter case, it these phenomena might be better appreciated as the boundaries of the passive characteristics of the normal healthy joint than negative attributes. For example, the healthy knee has been observed to have articular gaps in 90° of flexion in the medial compartment and in the lateral compartment depending on the posture.[16] The knee joint has long been known to possess an envelope of possible motions that only now are being explored by advanced measurement techniques.

The combination of dynamic imaging with flat-panel detectors and CT/MR bone models provide some novel measurement opportunities. However, refinements and enhancements to the method will expand the range of possible studies. First,

the flat-panel detector used for this study provided high spatial resolution but only three images/s. Solid-state detectors now commercially available with 30 images/s capabilities will permit study of highly dynamic activities. Second, single-plane imaging provides tremendous experimental flexibility and relatively large viewing volumes, but suffers from the main limitation of monocular vision—poor sensitivity for motions perpendicular to the image plane, which was approximately 2 mm in our preliminary study using a lower resolution image source.[5] Bi-plane imaging techniques can provide measurements with enhanced precision and more uniform uncertainties when required, but restrict the viewing volume, increase X-ray exposure and at least double the cost. Third, geometric and coordinate alignment errors in the CT and MR models affect the measurement accuracy, and it is well known that MR images/models suffer from geometric distortion.[5] For this reason, CT-derived models were used for 3D-to-2D model-to-image registration, only using the MR-derived models for articular surface analysis once the 3D pose of the bones was determined. In addition, the MR scans were performed nonweight bearing, so the compliant cartilage surfaces presumably were unloaded. Additional measurement uncertainty results when interrogating these cartilage surfaces based on weight-bearing conditions,[17] and the contact locations must be defined conservatively. Fourth, the current approach to analyzing joint contact ignores the menisci, which are invisible on X-ray but obviously affect joint contact and load distribution. There is not currently an X-ray-based technique that will overcome this limitation, but dynamic MR studies can provide this capability.[18] Finally, simple experimental issues limited the range of the current observations. Subjects were instructed to perform the three activities in a natural and comfortable manner, and some subjects extended and/or flexed their knees more than others. The data reported here are limited to the common flexion ranges for the subjects. In summary, the study provides observations of healthy knee kinematics in three different activities over the flexion range from extension to 150° using dynamic imaging with CT/MR-derived models. Future experimental and technical improvements might further expand the range and quality of measurements that can be obtained.

REFERENCES

1. Asano T, Akagi M, Tanaka K, et al. 2001. In vivo three-dimensional knee kinematics using a biplanar image-matching technique. Clin Orthop Relat Res 388:157–166.
2. Komistek RD, Dennis DA, Mahfouz M. 2003. In vivo fluoroscopic analysis of the normal human knee. Clin Orthop Relat Res 410:69–81.
3. Li G, DeFrate LE, Park SE, et al. 2005. In vivo articular cartilage contact kinematics of the knee: an investigation using dual-orthogonal fluoroscopy and magnetic resonance image based computer models. Am J Sports Med 33:102–107.
4. Fregly BJ, Rahman HA, Banks SA. 2005. Theoretical accuracy of model-based shape matching for measuring natural knee kinematics with single-plane fluoroscopy. J Biomech Eng 127:692–699.
5. Moro-oka T, Hamai S, Miura H, et al. 2007. Can MR derived bone models be used for accurate motion measurement with single-plane 3D shape registration? J Orthop Res 7:867–872.
6. Banks SA, Hodge WA. 1996. Accurate measurement of three-dimensional knee replacement kinematics using single-plane fluoroscopy. IEEE Trans Biomed Eng 43:638–649.
7. Tupling SJ, Pierrynowski MR. 1987. Use of cardan angles to locate rigid bodies in three-dimensional space. Med Biol Eng Comput 25:527–532.
8. Adam C, Eckstein F, Milz S, et al. 1998. The distribution of cartilage thickness in the knee-joints of old-aged individuals—measurement by A-mode ultrasound. Clin Biomech (Bristol, Avon) 13:1–10.
9. Koo S, Gold GE, Andriacchi TP. 2005. Considerations in measuring cartilage thickness using MRI: factors influencing reproducibility and accuracy. Osteoarthritis Cartilage 13:782–789.
10. Moglo KE, Shirazi-Adl A. 2005. Cruciate coupling and screw-home mechanism in passive knee joint during extension–flexion. J Biomech 38:1075–1083.
11. Iwaki H, Pinskerova V, Freeman MA. 2000. Tibiofemoral movement 1: the shapes and relative movements of the femur and tibia in the unloaded cadaver knee. J Bone Joint Surg Br 82:1189–1195.
12. Banks SA, Hodge WA. 2004. 2003 Hap Paul Award Paper of the International Society for Technology in Arthroplasty. Design and activity dependence of kinematics in fixed and mobile-bearing knee arthroplasties. J Arthroplasty 19:809–816.
13. Hill PF, Vedi V, Williams A, Iwaki H, et al. 2000. Tibiofemoral movement 2: the loaded and unloaded living knee studied by MRI. J Bone Joint Surg Br 82:1196–1198.
14. Karrholm J, Brandsson S, Freeman MA. 2000. Tibiofemoral movement 4: changes of axial tibial rotation caused by forced rotation at the weight-bearing knee studied by RSA. J Bone Joint Surg Br 82:1201–1203.
15. Nakagawa S, Kadoya Y, Todo S, et al. 2000. Tibiofemoral movement 3: full flexion in the living knee studied by MRI. J Bone Joint Surg Br 82:1199–1200.
16. Tokuhara Y, Kadoya Y, Nakagawa S, et al. 2004. The flexion gap in normal knees. An MRI study. J Bone Joint Surg Br 86:1133–1136.
17. Forster H, Fisher J. 1996. The influence of loading time and lubricant on the friction of articular cartilage. Proc Inst Mech Eng [H] 210:109–119.
18. Sheehan FT, Zajac FE, Drace JE. 1999. In vivo tracking of the human patella using cine phase contrast magnetic resonance imaging. J Biomech Eng 121:650–656.

Kinematic Analysis of Kneeling in Cruciate-Retaining and Posterior-Stabilized Total Knee Arthroplasties

Satoshi Hamai,[1] Hiromasa Miura,[1] Hidehiko Higaki,[2] Shuichi Matsuda,[1] Takeshi Shimoto,[2] Kousuke Sasaki,[1] Masaaki Yoshizumi,[2] Ken Okazaki,[1] Nobuaki Tsukamoto,[1] Yukihide Iwamoto[1]

[1]Department of Orthopaedic Surgery, Graduate School of Medical Sciences, Kyushu University, 3-1-1 Maidashi, Higashi-ku, Fukuoka 812-8582, Japan

[2]Department of Mechanical Engineering, Faculty of Engineering, Kyushu Sangyo University, 2-3-1 Matsugadai, Higashi-ku, Fukuoka 813-8583, Japan

Received 17 August 2006; accepted 26 July 2007

Published online in Wiley InterScience (www.interscience.wiley.com). DOI 10.1002/jor.20512

ABSTRACT: Kneeling is an important function of the knee for many activities of daily living. In this study, we evaluated the in vivo kinematics of kneeling after total knee arthroplasty (TKA) using radiographic based image-matching techniques. Kneeling from 90 to 120° of knee flexion produced a posterior femoral rollback after both cruciate-retaining and posterior-stabilized TKA. It could be assumed that the posterior cruciate ligament and the post-cam mechanism were functioning. The posterior-stabilized TKA design had contact regions located far posterior on the tibial insert in comparison to the cruciate-retaining TKA. Specifically, the lateral femoral condyle in posterior-stabilized TKA translated to the posterior edge of the tibial surface, although there was no finding of subluxation. After posterior-stabilized TKA, the contact position of the post-cam translated to the posterior medial corner of the post with external rotation of the femoral component. Because edge loading can induce accelerated polyethylene wear, the configuration of the post-cam mechanism should be designed to provide a larger contact area when the femoral component rotates. © 2007 Orthopaedic Research Society. Published by Wiley Periodicals, Inc. J Orthop Res 26:435–442, 2008

Keywords: kinematics; kneeling; posterior cruciate ligament; post-cam mechanism; total knee arthroplasty

INTRODUCTION

Kneeling is an important function for many activities of daily living. More than 50% of all patients undergoing total knee arthroplasty (TKA) consider kneeling important and participate in kneeling.[1] Inability to kneel after knee surgery is a frequent cause of dissatisfaction. Kneeling for different functions requires different degrees of knee flexion. Kneeling in 90° of knee flexion has been called "upright kneeling" and kneeling in more than 110° of knee flexion "flexed kneeling."[2] Flexed kneeling is important especially in Middle and Far Eastern patients as they sit on and rise from the floor. The patella and the tibial tuberosity contact the ground in upright kneeling, while only the tibial tuberosity bears weight in flexed kneeling.[3]

Kneeling ability depends on many factors. Scar position and skin hypoesthesia can limit kneeling ability. A lateral incision produces less dysesthesia, fewer neuromas, and less discomfort.[4] A patient's ability to kneel may be greater than their own perception of their ability to do so.[2,5] Many patients undergoing TKA avoid kneeling for fear of harming the prosthesis.

Weight-bearing load may be exerted on the patellofemoral articulation and the retained posterior cruciate ligament (PCL) after cruciate-retaining (CR) TKA or the post-cam mechanism after posterior-stabilized (PS) TKA during activities requiring deep flexion.[6–8] However, very little is known regarding knee kinematics during upright and flexed kneeling, and even less is known about how TKA design affects knee biomechanics at this limit of knee flexion. The purpose of this study was to clarify in vivo knee kinematics during kneeling. In addition, we compared kinematics with the joint in a hyperflexed position between CR TKA and PS TKA.

The in vivo 3D position and orientation of the components of CR and PS TKA during both upright and flexed kneeling were evaluated using an image-matching method. In a previous study, Komistek et al.[9] analyzed femorotibial contact positions in static upright kneeling using an iterative computer model-fitting technique. However,

Correspondence to: Hiromasa Miura (Telephone: +81-92-642-5488; Fax: +81-92-642-5507; E-mail: miura@ortho.med.kyushu-u.ac.jp)

little information is available on the in vivo dynamic kinematics of kneeling from 90 to 120° of flexion after TKA.[10] In addition, this study analyzed subjects having a PS TKA to determine the contact position at the post-cam mechanism. Nakayama et al.[11] measured in vitro contact areas and stresses at the post-cam mechanism using a digital electric stress sensor. However, in vivo post-cam contact positions after PS TKA have not been reported.

We hypothesized that knee flexion angles and type of TKA design would affect the tibiofemoral contact positions during kneeling, and that the post-cam contact position after PS TKA would not be in the center of the post at flexed positions.

MATERIALS AND METHODS

Twenty subjects who had undergone clinically successful TKA and were willing to participate enrolled in the study. Inclusion criteria were the ability to perform both upright and flexed kneeling. All subjects gave informed consent, and an institutional review board approved the study. Ten knees in eight subjects received CR TKA (Foundation knee, Encore Medical Co., Austin, TX) and 10 knees in seven subjects received PS TKA (Nexgen LPS, Zimmer, Inc., Warsaw, IN). The articulating surface geometry of the polyethylene tibial insert is conforming in PS TKA, but relatively flat in CR TKA, allowing femoral rollback produced by tensioning of the PCL during flexion.

The 20 subjects included 18 women and 2 men with an average follow-up of 17.3 months. The preoperative diagnoses were osteoarthritis in 15 knees and rheumatoid arthritis in 5, and the average age at surgery was 71.6 years. Average postoperative knee extension/flexion angle was −2.8/128.4°. The Knee Society score (knee score/function score) was 91.4/80.6. Three experienced surgeons (H.M., S.M., and K.O.) performed all TKAs using a similar standard technique. The components were aligned so that the mechanical axis passed through the center of the knee prosthesis. Rotational alignment was adjusted to bony landmarks, such as the transepicondylar axis and tibial tuberosity. The PCL was retained when it appeared normal in tension and appearance at surgery. Soft tissues were balanced to achieve varus and valgus stability.

Each subject was asked to perform upright and flexed kneeling in maximum knee flexion under radiological surveillance (Fig. 1). Knee flexion in each subject reached more than 120° of knee flexion passively. During kneeling, subjects placed their leg on a box with the ankle joint extended. Continuous X-ray images were taken using a flat panel detector (Clavis, Hitachi, Co., Ltd., Tokyo). The detector provided higher resolution dynamic images (Distortion-free image, 0.20 × 0.20 mm/pixel resolution, three frames/s, with an image area size 397 (H) × 298 (V) mm). The high contrast resolution of X-ray images provided the basis for the required accuracy.[12,13] Images of kneeling at 90, 100, 110, and 120° of flexion were selected from the continuous images and analyzed using a previously published image-matching technique.[14,15]

The projected 3D computer-aided design (CAD) models of the femoral and tibial components were superimposed on the 2D radiographic images (Fig. 2a). The 3D CAD models of the components and the tibial insert were reconstructed after 3D shape measurements of the total knee prostheses by a profilometer (Mitsutoyo, Co., Ltd., Kawasaki, Japan) (Fig. 2b). The position of the radiation source relative to the X-ray detector was determined from the projection image of a calibration cage made from an acrylic resin board and metallic balls. Projecting all surface points of the 3D model produced the component silhouette. A model silhouette was matched with the actual silhouette by translating and rotating the 3D CAD model to minimize the number of unmatched pixels between the silhouettes. After the 3D pose of the components was estimated, the 6 degrees of freedom of the femoral component relative to the tibial component were determined by transforming the coordinate systems into one common system.

The accuracy and precision of the measurement technique was determined by in vitro investigations.[15,16]

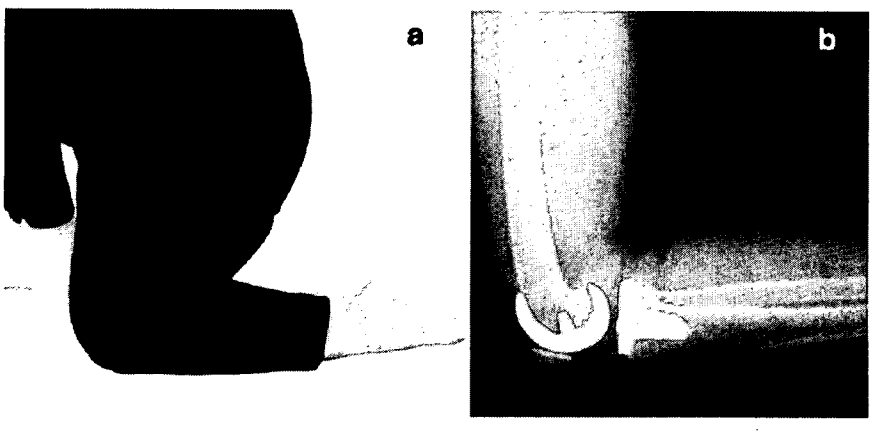

Figure 1. Each subject was asked to perform kneeling from 90° to maximum knee flexion (a). Continuous X-ray images of kneeling were taken using a flat panel detector (b).

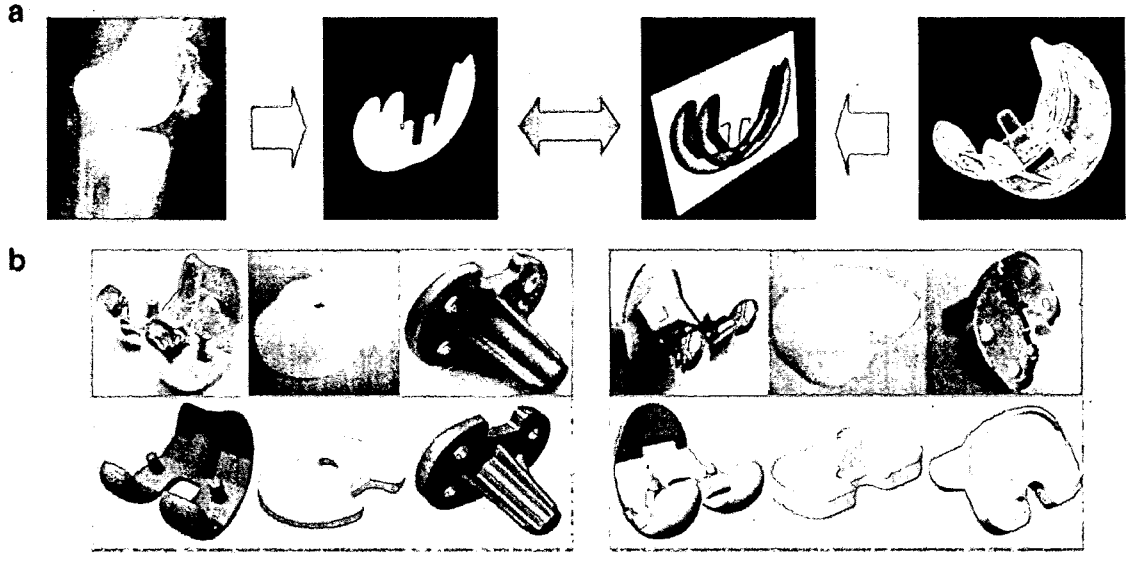

Figure 2. A model silhouette was matched with the actual object silhouette by translating and rotating the 3D CAD models (a). The models of the components (lower stand) were reconstructed at CR TKA (left) and PS TKA (right) after 3D shape measurements of the total knee prostheses (upper stand) by a profilometer (b).

The components mounted on a stage were rotated and translated to known values. The image-matching process was performed for the radiographic images at each position to determine the relative pose of the components. The root-mean-square (RMS) accuracy errors for this process for the femoral component were 0.29 mm for in-plane translation, 0.37 mm for out-of-plane translation, and 0.27° for rotation, and the accuracies for the tibial component were 0.23 mm for in-plane translation, 0.30 mm for out-of-plane translation, and 0.25° for rotation. The maximum errors associated with tracking the position of the tibia relative to the femur were the sum of the RMS errors, which were 0.52, 0.67 mm, and 0.52° respectively, for in-plane and out-of-plane translations and rotation.

The contact positions between the femoral component and tibial insert and tibiofemoral axial rotation were evaluated after both CR and PS TKA (Fig. 3). The contact positions were evaluated by measuring the centroid of contact area between the surfaces of the femoral condyles and the insert using a CAD software program (SolidWorks® 2001Plus SP3.0, SolidWorks Corporation, Concord, MA) (Fig. 3a). If surface separation was recognized, the location of closest proximity between the surfaces of the femoral condyles and the insert was measured in 3D space. The positive or negative value of AP tibiofemoral contact position was defined as anterior or posterior to the midline of the polyethylene insert. The tibiofemoral rotation was evaluated to measure the rotation angle of the femoral component relative to the tibial component (Fig. 3b). The positive or negative value of tibiofemoral rotation was defined as internal or external rotation of the femur relative to tibia. After PS TKA, the medial–lateral and upper–lower translation of contact position between the femoral cam and tibial post was evaluated (Fig. 3c). The positive or negative value of ML post-cam contact position was defined as medial or lateral to the center of the post. The positive or negative value of proximal–distal post-cam contact position was defined as proximal or distal to the most inferior point of the articular surface.

Statistical analyses were done using Stat View 5.0 (Abacus Concepts, Inc., Berkeley, CA). All values were expressed as the mean ± standard deviation. The unpaired t-test was used to analyze postoperative knee extension/flexion angles and the Knee Society scores (knee score/function score) comparing CR with PS TKA. Two-way, repeated measures ANOVA were used to analyze the tibiofemoral contact positions and tibiofemoral rotations when investigating the effects of knee flexion angle and TKA design and a comparison of the interaction between these two values. Post hoc tests (Bonferroni/Dunn) were used to identify the source of any differences for relevant comparisons. The paired t-test was used to analyze the ML post-cam contact position when comparing 90° with 120° of flexion. A value of $p < 0.05$ was considered significant.

RESULTS

The average postoperative extension/flexion angle was $-3.8 \pm 2.5°/129.3 \pm 5.4°$ after CR TKA and $-2.0 \pm 3.3°/127.7 \pm 8.6°$ after PS TKA. No significant differences were found in postoperative knee extension ($p = 0.24$) and flexion ($p = 0.66$) between CR TKA and PS TKA. The Knee Society score (knee score/function score) was $90 \pm 6.3/78 \pm 11.6$

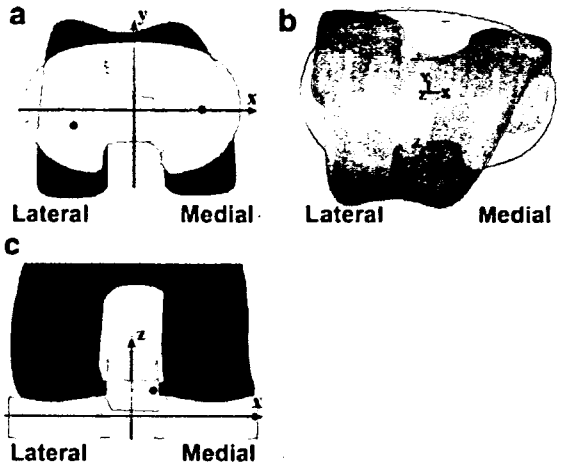

Figure 3. (a) Locations of closest proximity or contact between the femoral component and the tibial insert on the medial and lateral sides. The positive or negative value of the AP tibiofemoral contact position was defined as anterior or posterior to the midline of the tibial insert. (b) The rotation angle of the femoral component relative to the tibial component. The positive or negative value of tibiofemoral rotation was defined as internal or external rotation of the femur relative to tibia. (c) Location of contact between the femoral cam and tibial post after PS TKA. The positive or negative value of medial–lateral post-cam contact position was defined as medial or lateral to the center of the post. The positive or negative value of proximal–distal post-cam contact was defined as proximal or distal to the most inferior point of the articular surface.

for CR and $93 \pm 5.7/82 \pm 13.8$ for PS TKA. No significant differences (knee score: $p = 0.27$; function score: $p = 0.59$) were found between CR TKA and PS TKA.

The average AP tibiofemoral contact positions in 90° of flexion after PS TKA were significantly ($p < 0.0001$) more posterior than after CR TKA with both condyles (Table 1 and Fig. 4). Kneeling from 90 to 120° of flexion produced a posterior femoral rollback for both designs. Anterior femoral translation was not found for any subject from 90 to 120° of flexion. A significant interaction was found between flexion position and TKA design (ANOVA, $p < 0.01$), indicating that the pattern of changes during kneeling differed between TKA designs. The total rollback after PS TKA (medial = -5.2 ± 2.4 mm, range -1.1 to -8.5 mm; lateral = -4.8 ± 3.2 mm, range -0.3 to -10.1 mm) was more than after CR TKA (medial = -4.3 ± 3.7 mm, range -0.1 to -11.4 mm; lateral = -2.4 ± 1.4 mm, range -0.3 to -4.4 mm) with both condyles. The average AP tibiofemoral contact positions in 120° of flexion after PS TKA were significantly ($p < 0.0001$) more posterior than after CR TKA with both condyles (Table 1).

Changes in the rotation angle from 90 to 120° of flexion were $0.4 \pm 2.5°$ (range -2.8 to 4.4°) after CR TKA and $-1.3 \pm 0.8°$ (range -2.3 to $-0.1°$) after PS TKA. After PS TKA, the change in the external rotation was consistently recognized in each 10° of flexion. The rotation angle in 120° of flexion was $-7.5 \pm 5.4°$ (range -15.7 to $-0.5°$) after CR TKA and $-6.9 \pm 4.1°$ (range -12.9 to $-2.1°$) at PS TKA. The femoral components for both designs continued to show external rotation from 90° to 120° of flexion. More than 10° of the external rotation was recognized during kneeling for both designs (CR, 4; PS, 3).

The average ML post-cam contact position in 90° of flexion was 4.0 ± 2.2 mm (range 0.1 to 6.1 mm) medial from the center of the post with external rotation of the femoral component (Table 1 and Fig. 4c). 1.2 ± 1.2 mm (range 0.1 to 3.4 mm) medial translation of the post-cam contact position occurred from 90 to 120° of flexion because the femoral component rotated externally. The average ML post-cam contact position in 120° of flexion was significantly more medial than in 90° ($p < 0.05$). The average proximal–distal post-cam contact position in 90° of flexion was proximal from the most inferior point of the articular surface (Table 1 and Fig. 4c). 1.4 ± 0.9 mm (range 0.0 to 2.4 mm) distal translation of the post-cam contact position occurred from 90 to 120° of flexion. No proximal translation was observed from 90 to 120° of knee flexion.

DISCUSSION

Kneeling in more than 110° of knee flexion tends to produce posterior translation of the tibia relative to the femur because the tibial tuberosity bears weight.[2] The ground reaction force on the tibial tuberosity causes a posterior directed shear force on the tibia during kneeling. However, posterior translation is prevented by the retained PCL after CR TKA and the post-cam mechanism after PS TKA. Without PCL retention or the post-cam mechanism, the femoral component would not rollback posteriorly, instead translating anteriorly. If the retained PCL and the post-cam mechanism did not provide posterior rollback, an excessive patellofemoral contact force may occur. In this study, kneeling from 90 to 120° of flexion produced posterior rollback in both designs (Fig. 4a and b). Previous studies reported that the retained PCL after CR TKA reproduces posterior rollback.[17–20] In addition, after PS TKA, the post-cam mechanism was designed to function over 75° of knee flexion, so we can assume

Table 1. AP Tibiofemoral Contact Positions [+ Anterior, − Posterior] and Tibiofemoral Rotation [+ IR, − ER] after Both CR and PS TKA, and the ML [+ Medial, − Lateral] and Proximal-Distal [+ Proximal from the Most Inferior Point of the Articular Surface] Post-cam Contact Position after PS TKA while Kneeling from 90° to 120° of Knee Flexion

	AP Tibiofemoral Contact Positions (mm)	
Cruciate-retaining TKA	Medial Condyle/Lateral Condyle	Rotation (°)
90°	$4.2 \pm 3.6^a/-4.8 \pm 3.3^a$	-7.8 ± 4.8
100°	$2.6 \pm 2.5^a/-5.4 \pm 3.4^a$	-7.6 ± 4.7
110°	$1.1 \pm 2.8^a/-6.1 \pm 3.4^a$	-7.5 ± 5.3
120°	$-0.1 \pm 3.3^a/-7.2 \pm 3.9^a$	-7.5 ± 5.4
	ML Tibiofemoral Contact Positions (mm)	
Posterior-stabilized TKA	Medial Condyle/Lateral Condyle	Rotation (°)
90°	$-3.7 \pm 3.2^a/-10.5 \pm 3.3^a$	-5.6 ± 4.2
100°	$-5.8 \pm 4.1^a/-12.2 \pm 1.9^a$	-5.9 ± 4.2
110°	$-7.6 \pm 4.1^a/-14.3 \pm 1.2^a$	-6.4 ± 4.1
120°	$-8.9 \pm 4.6^a/-15.3 \pm 2.1^a$	-6.9 ± 4.1
	Post-cam Contact Position (mm)	
Posterior-stabilized TKA	Medial–lateral/Proximal–distal	
90°	$4.0 \pm 2.2/7.6 \pm 0.7$	
100°	$4.3 \pm 2.3/6.9 \pm 0.5$	
110°	$4.7 \pm 1.5/6.3 \pm 0.7$	
120°	$5.1 \pm 1.2/6.2 \pm 0.8$	

Values are mean ± standard deviation.
[a]Significantly different between CR TKA and PS TKA ($p < 0.05$).

that both the retained PCL and the post-cam mechanism were functioning.

Posterior femoral rollback was preferable to decrease patellofemoral contact force during kneeling. Increased femoral rollback in flexion correlates with reduced patellofemoral contact load in TKA.[21] This reduction in contact force is attributed to the increased extensor moment arm. Browne et al.[22] reported that the design with the longer extensor moment arm required less quadriceps force and reduced patellofemoral compressive force. In PS TKA, contact positions at 90° of flexion were more posterior, and rollback distance with both condyles was longer compared to CR TKA. PS TKA may be preferable to CR TKA to reduce patellofemoral forces during kneeling. Komistek et al.[9] found similar results using in vivo fluoroscopy to evaluate femorotibial contact positions in upright kneeling, reporting that the PCL has less resistance to the anterior thrust of the femur relative to the tibia in PS TKA.

The PS design had contact regions located more posterior on the tibial insert in comparison to the CR design. Specifically, the lateral femoral condyle in the PS translated to the posterior edge of the tibial surface during kneeling, although subluxation did not occur. This finding has important implications regarding the location and severity of the polyethylene wear. The posteromedial corner of the lateral compartment of the tibial insert suffered edge loading by combining posterior translation and external rotation of the femoral component during kneeling. Wasielewski et al.[23] and Harman et al.[24] showed wear patterns on retrieved polyethylene insert consistent with these articular contact patterns. The contact locations between the femoral component and polyethylene insert during dynamic activities are thus considered to

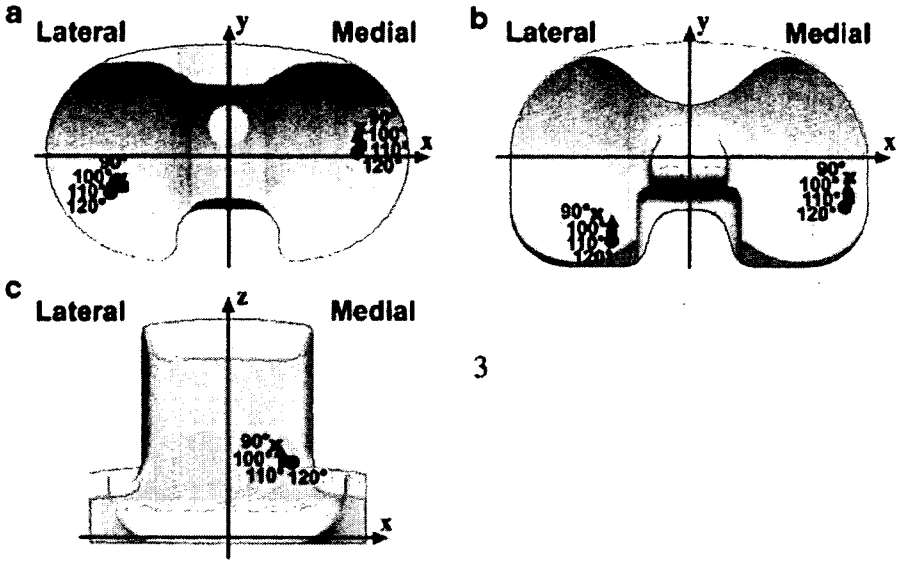

Figure 4. The average tibiofemoral contact positions after CR TKA (a) and PS TKA (b) demonstrated posterior roll back during kneeling from 90 to 120° of knee flexion. The average post-cam contact position after PS TKA translated medially and downward during kneeling (c).

correspond to the wear pattern on the polyethylene articular surface.

No in vivo studies have yet focused on the post-cam contact positions in PS TKA. The post-cam contact position during kneeling translated medially and distally along the post (Fig. 4c). The effect of femoral rotation is important for the ML post-cam contact position. External rotation of the femoral component from 90 to 120° of flexion created a medial translation of the post-cam contact position (Fig. 5). Furthermore, 3 of 10 knees after PS TKA had more than 10° of femoral external rotation during kneeling with the risk that the posterior medial corner of the flat-surfaced post could suffer excessive stress because of edge loading. Nakayama et al.[11] reported that when the tibial component was rotated 10°, post-cam contact stress increased more than twofold in comparison to neutral rotation. Edge loading may cause chronic wear and fracture of the post, affecting the long-term prognosis following TKA. The post-cam design should be modified to provide a larger contact area and prevent increased contact stress when the femoral component rotates.

Distal translation of the post-cam contact position was found during kneeling. Condylar liftoff is an important issue for proximal–distal post-cam contact position. However, the proximal–distal post-cam contact position demonstrated no proximal translation. The distal translation is more beneficial in preventing posterior dislocation of the tibial component and in decreasing the risk of fracture of the post. If flexion instability exists after PS TKA, posterior dislocation of the tibial component may occur.[25–28] However, none of the subjects in this study had evidence of ligamentous laxity or pain on physical examination.

We are concerned about the effect of the load that is exerted on the post-cam mechanism during kneeling. Fracture or polyethylene wear of the post and dislocation of the knee have been reported after PS TKA.[25–33] In addition, the post-cam mechanism could transmit anteroposterior shear and tensile stresses to the bone–implant interfaces and cause component loosening. After CR TKA, the PCL would play a role in dissipating shear and tensile stresses on the bone–implant interfaces.[34] However, further

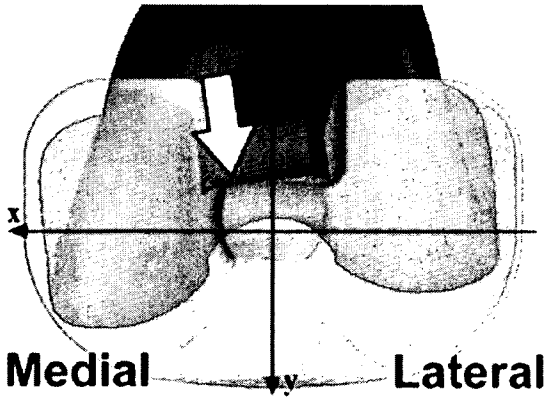

Figure 5. The contact position of the post-cam translated to the posterior medial corner of the post with the external rotation of the femoral component (arrow).

studies are needed to examine changes in PCL laxity due to degeneration or attenuation with time. Flexion instability due to late PCL insufficiency could be a cause of persistent pain and functional impairment after CR TKA leading to revision arthroplasty.[35–37] Frequent kneeling may cause a dysfunction of the retained PCL after CR TKA and the post-cam mechanism after PS TKA over time because the retained PCL and the post-cam mechanism receive significant load.

Our study has limitations. Kinematic information concerning deep knee flexion could not be included in the analysis because most of the subjects could not kneel beyond 130°. Both CR and PS designs used in this study are not intended to flex beyond 130°. More research is needed to assess the dynamic in vivo function of the PCL and the post-cam mechanism in deep flexion.

In conclusion, our results suggest that the PCL after CR TKA and the post-cam mechanism after PS TKA function during kneeling from 90 to 120° of knee flexion. Based on our results, PS TKA may be preferable to CR TKA to reduce forces across the patellofemoral articulation. The PS design has contact regions located far posterior on the tibial insert in comparison to the CR TKA. Specifically, the lateral femoral condyle in PS TKA translated to the posterior edge of the tibial surface. Furthermore, this study suggests the hypothesis that increased edge loading may be associated with an abnormally high degree of stress in the polyethylene, and that this may be associated with an increased risk of failure. Only a clinical study with long term follow-up can determine if this relationship exists, but further attention must be given to the configuration of the post-cam when designing posterior-stabilized total knee prostheses.

ACKNOWLEDGMENTS

No benefits in any form were received from a commercial party related directly or indirectly to the subject of this article.

REFERENCES

1. Weiss JM, Noble PC, Conditt MA, et al. 2002. What functional activities are important to patients with knee replacements? Clin Orthop 404:172–188.
2. Palmer SH, Servant CT, Maguire J, et al. 2002. Ability to kneel after total knee replacement. J Bone Joint Surg Br 84:220–222.
3. Hassaballa M, Vale T, Weeg N, et al. 2002. Kneeling requirements and arthroplasty surgery. Knee 9:317–319.
4. Berg P, Mjoberg B. 1991. A lateral skin incision reduces peripatellar dysaesthesia after knee surgery. J Bone Joint Surg Br 73:374–376.
5. Schai PA, Gibbon AJ, Scott RD. 1999. Kneeling ability after total knee arthroplasty. Perception and reality. Clin Orthop 367:195–200.
6. Dahlkvist NJ, Mayo P, Seedhom BB. 1982. Forces during squatting and rising from a deep squat. Eng Med 11:69–76.
7. Toutoungi DE, Lu TW, Leardini A, et al. 2000. Cruciate ligament forces in the human knee during rehabilitation exercises. Clin Biomech 15:176–177.
8. Nagura T, Dyrby CO, Alexander EJ, et al. 2002. Mechanical loads at the knee joint during deep flexion. J Orthop Res 20:881–886.
9. Komistek RD, Scott RD, Dennis DA, et al. 2002. In vivo comparison of femorotibial contact positions for press-fit posterior stabilized and posterior cruciate-retaining total knee arthroplasties. J Arthroplasty 17:209–216.
10. Incavo SJ, Mullins ER, Coughlin KM, et al. 2004. Tibiofemoral kinematic analysis of kneeling after total knee arthroplasty. J Arthroplasty 19:906–910.
11. Nakayama K, Matsuda S, Miura H, et al. 2005. Contact stress at the post-cam mechanism in posterior-stabilized total knee arthroplasty. J Bone Joint Surg Br 87:483–488.
12. Garling EH, Kaptein BL, Geleijns K, et al. 2005. Marker configuration model-based roentgen fluoroscopic analysis. J Biomech 38:893–901.
13. Fukuoka Y, Hoshino A, Ishida A. 1999. A simple radiographic measurement method for polyethylene wear in total knee arthroplasty. IEEE Trans Rehabil Eng 7:228–233.
14. Banks SA, Hodge WA. 1996. Accurate measurement of three-dimensional knee replacement kinematics using single-plane fluoroscopy. IEEE Trans Biomed Eng 43: 638–649.
15. Higaki H, Shimoto T, Miura H, et al. 2002. Application of pattern matching method in motion analysis for TKA. Trans Jpn Soc Mech Eng 68:3061–3068.
16. Shimoto T, Higaki H, Hukunaga T, et al. 2003. Study of the motion analysis for total knee arthroplasty using flat panel detector. Proceedings of the IASTED International Conference on Biomechanics. Calgary, Canada: ACTA Press; p 28–33.
17. Hazaki S, Yokoyama Y, Inoue H. 2001. A radiographic analysis of anterior–posterior translation in total knee arthroplasty. J Orthop Sci 6:390–396.
18. Bertin KC, Komistek RD, Dennis DA, et al. 2002. In vivo determination of posterior femoral rollback for subjects having a NexGen posterior cruciate-retaining total knee arthroplasty. J Arthroplasty 17:1040–1048.
19. Nozaki H, Banks SA, Suguro T, et al. 2002. Observations of femoral rollback in cruciate-retaining knee arthroplasty. Clin Orthop 404:308–314.
20. Most E, Zayontz S, Li G, et al. 2003. Femoral rollback after cruciate-retaining and stabilizing total knee arthroplasty. Clin Orthop 410:101–113.
21. Churchill DL, Incavo SJ, Johnson CC, et al. 2001. The influence of femoral rollback on patellofemoral contact loads in total knee arthroplasty. J Arthroplasty 16:909–918.
22. Browne C, Hermida JC, Bergula A, et al. 2005. Patellofemoral forces after total knee arthroplasty: effect of extensor moment arm. Knee 12:81–88.
23. Wasielewski RC, Galante JO, Leighty RM, et al. 1994. Wear patterns on retrieved polyethylene tibial inserts and

their relationship to technical considerations during total knee arthroplasty. Clin Orthop 299:31–43.
24. Harman MK, Banks SA, Hodge WA. 2001. Polyethylene damage and knee kinematics after total knee arthroplasty. Clin Orthop 392:383–393.
25. Gidwani S, Langkamer VG. 2001. Recurrent dislocation of a posterior-stabilized prosthesis: a series of three cases. Knee 8:317–320.
26. Ochsner JL Jr, Kostman WC, Dodson M. 1996. Posterior dislocation of a posterior-stabilized total knee arthroplasty. A report of two cases. Am J Orthop 25:310–312.
27. Petrie RS, Trousdale RT, Cabanela ME. 2000. Total knee arthroplasty for chronic posterior knee dislocation: report of 2 cases with technical considerations. J Arthroplasty 15:380–386.
28. Su YP, Chiu FY, Chen TH. 2003. Posterior dislocation after posterior stabilization TKA. J Chin Med Assoc 66:120–122.
29. Clarke HD, Math KR, Scuderi GR. 2004. Polyethylene post failure in posterior stabilized total knee arthroplasty. J Arthroplasty 19:652–657.
30. Hendel D, Garti A, Weisbort M. 2003. Fracture of the central polyethylene tibial spine in posterior stabilized total knee arthroplasty. J Arthroplasty 18:672–674.
31. Mestha P, Shenava Y, D'Arcy JC. 2000. Fracture of the polyethylene tibial post in posterior stabilized (Insall Burstein II) total knee arthroplasty. J Arthroplasty 15: 814–815.
32. Ng TP, Chiu KY. 2003. Recurrent dislocation of total knee arthroplasty: an unusual cause. J Arthroplasty 18:1067–1070.
33. Puloski SK, McCalden RW, MacDonald SJ, et al. 2001. Tibial post wear in posterior stabilized total knee arthroplasty. An unrecognized source of polyethylene debris. J Bone Joint Surg Am 83:390–397.
34. Andriacchi TP, Galante JO. 1988. Retention of the posterior cruciate in total knee arthroplasty. J Arthroplasty 3 (Suppl):S13–S19.
35. Montgomery RL, Goodman SB, Csongradi J. 1993. Late rupture of the posterior cruciate ligament after total knee replacement. Iowa Orthop J 13:167–170.
36. Pagnano MW, Hanssen AD, Lewallen DG, et al. 1998. Flexion instability after primary posterior cruciate retaining total knee arthroplasty. Clin Orthop 356:39–46.
37. Wang CJ, Wang HE. 1997. Dislocation of total knee arthroplasty. A report of 6 cases with 2 patterns of instability. Acta Orthop Scand 68:282–285.

Can Magnetic Resonance Imaging–Derived Bone Models Be Used for Accurate Motion Measurement with Single-Plane Three-Dimensional Shape Registration?

Taka-aki Moro-oka,[1,2,3] Satoshi Hamai,[3] Hiromasa Miura,[3] Takeshi Shimoto,[4] Hidehiko Higaki,[4] Benjamin J. Fregly,[1] Yukihide Iwamoto,[3] Scott A. Banks[1,5]

[1]Department of Mechanical & Aerospace Engineering, University of Florida, 318 MAE-A, Mail Stop 116250, Gainesville, Florida 32611-6250

[2]Seimeikai Moro-oka Orthopaedic Hospital, Fukuoka, Japan

[3]Department of Orthopaedic Surgery, Graduate School of Medical Sciences, Kyushu University, Fukuoka, Japan

[4]Department of Mechanical Engineering, Faculty of Engineering, Kyushu Sangyo University, Fukuoka, Japan

[5]The BioMotion Foundation, Palm Beach, Florida

Received 30 March 2006; accepted 8 November 2006

Published online 8 February 2007 in Wiley InterScience (www.interscience.wiley.com). DOI 10.1002/jor.20355

ABSTRACT: The purpose of this study was to compare three-dimensional (3D) kinematic measurements from single-plane radiographic projections using bone models created from magnetic resonance imaging (MRI) and computed tomography (CT). MRI is attractive because there is no ionizing radiation, but geometric field distortion and poor bone contrast degrade model fidelity compared to CT. We created knee bone models of three healthy volunteers from both MRI and CT and performed three quantitative comparisons. First, differences between MRI– and CT–derived bone model surfaces were measured. Second, shape matching motion measurements were done with bone models for X-ray image sequences of a squat activity. Third, synthetic X-ray images in known poses were created and shape matching was again performed. Differences in kinematic results were quantified in terms of root mean square (RMS) error. Mean differences between CT and MRI model surfaces for the femur and tibia were −0.08 mm and −0.14 mm, respectively. There were significant differences in three of six kinematic parameters comparing matching results from MRI–derived bone models and CT–derived bone models. RMS errors for tibiofemoral poses averaged 0.74 mm for sagittal translations, 2.0 mm for mediolateral translations, and 1.4° for all rotations with MRI models. Average RMS errors were 0.53 mm for sagittal translations, 1.6 mm for mediolateral translations, and 0.54° for all rotations with the CT models. Single-plane X-ray imaging with model-based shape matching provides kinematic measurements with sufficient accuracy to assess knee motions using either MRI– or CT–derived bone models. However, extra care should be taken when using MRI–derived bone models because model inaccuracies will affect the quality of the shape matching results. © 2007 Orthopaedic Research Society. Published by Wiley Periodicals, Inc. J Orthop Res 25:867–872, 2007

Keywords: magnetic resonance imaging (MRI); image distortion; computed tomography (CT); three-dimensional kinematics; knee

INTRODUCTION

Shape matching techniques have been used for 15 years to determine knee arthroplasty motions from fluoroscopic image sequences.[1–3] Recently, these techniques have been applied for motion measurement in joints without metallic implants, where three-dimensional (3D) surface models of the bones are created from magnetic resonance imaging (MRI)[4] and computed tomography (CT).[2,5–7] However, we are unaware of any rigorous assessment of the use of MRI–derived models for the purpose of shape registration–based motion measurement. DeFrate and colleagues reported the advantages of MRI-based model creation included the ability to add cartilage to the models and to avoid radiation exposure, but they did not directly assess the accuracy of their

Correspondence to: Scott A. Banks (Telephone: 352-392-6109; Fax: 352-392-7303; E-mail: banks@ufl.edu)

shape matching technique using the MRI–derived bone models.[4,8] It is well recognized that MRI provides lower bone contrast than CT and suffers from spatial distortions which vary by scanner, scan sequence, and the object being scanned.[9–18] MRI use is limited, for example, in stereotactic surgery of the brain unless geometric distortion correction has been performed.[14,15] Similarly, shape registration–based motion measurement requires submillimeter model accuracy for many clinically relevant measurement scenarios. In contrast, CT has negligible scaling error because images are reconstructed from line-of-sight X-ray optics.[9,11,13] The purposes of this study were to compare 3D kinematics from model-based shape matching using CT– and MRI–derived bone models and to determine if MRI–derived bone models provide sufficient fidelity to provide clinically relevant measurements.

METHODS

Three healthy subjects gave informed consent to participate in this study as approved by the institutional review board. Geometric bone models of the femur and tibia/fibula were created from CT (Toshiba, Aquilion, Tochigi, Japan) and MRI (Hitachi, Airis II Comfort, 0.3 T, Tokyo, Japan) scans of one leg. CT scans used a 512 × 512 image matrix, a 0.35 × 0.35 pixel dim, and a 1.00-mm thickness spanning approximately 150 mm above and below the joint line of the knee, and 2-mm slices through the centers of the hip and ankle joints. CT scan time was 49 s. MRI scans used a 512 × 512 image matrix, a 0.39 × 0.39 pixel dim, and a 1.0-mm thickness spanning more than 80 mm above and below the joint line of the knee. The MRI protocol was 3DT1GE, RF spoiled SARGE(RSSG). MR scan time ranged from 11 to 15 min.

Exterior cortical bone edges were segmented using commercial software (SliceOmatic, Tomovision, Montreal, CA), and these point clouds were converted into polygonal surface models (Geomagic Studio, Raindrop Geomagic, Research Triangle Park, NC). Interior cortical bone edges were not included because of poor definition in the epiphyseal and metaphyseal regions.

Anatomical coordinate systems were embedded in each bone model following a combination of previous approaches.[5,19,20] The coordinate systems were first defined for the CT models. The mediolateral (x) axes of the femur and tibia/fibula were defined by fitting a cylinder to each posterior condyle of the femur. The midpoint of the cylindrical axis was defined as the origin. The proximal/distal (y) axis for the femur was defined by a line perpendicular to the cylindrical axis in the plane intersecting the femoral head center. The proximal/distal (y) axis for the shank was perpendicular to the cylindrical axis in the plane intersecting the ankle center. The anteroposterior (z) axis was formed from the cross product of the first two. Next, the MRI model was registered with the corresponding CT model in its initial reference pose to align the embedded coordinate systems in each bone model. Automated alignment software was used with a proprietary algorithm to match 3D surfaces (Geomagic Studio). Fitting results were accurate to less than 0.1 microns in length and 0.1 arc seconds (1/36,000 of a degree) in angle compared to the official reference value.

The CT models were then shortened to the same length as the MRI models. Three experiments were performed to compare the CT and MR models.

Experiment 1

Differences between MRI and CT model surfaces were measured using inspection software (Geomagic Studio).

Experiment 2

Shape matching with the CT– and MRI–derived models was performed independently, without any information from one kinematic solution affecting the kinematic solution of the other. Continuous X-ray images of a squat activity for each subject were taken using a flat panel detector [Hitachi, Clavis, Tokyo, Japan; 3 frames/s, image area size 397 (H) × 298 (V) mm, and 0.20 × 0.20 mm/pixel resolution]. These images were scaled to 512 × 512 square pixels for 3D shape registration. A Canny edge detector was used to identify bony contours. At first, bone models were aligned manually by the order of 0.27 mm for in-plane translations, 0.95 mm for out-of-plane translation, and 0.25° for rotation. Next, an automated matching algorithm, based on nonlinear least squares optimization and an image edge-to-model edge distance criteria, was used to align both sets of bone models to 22 X-ray images for each knee (Fig. 1a). The computation time for the matching algorithm was 10 to 20 s per model (Dell precision 650, Intel Xeon processor, 2.40 GHz, 1.00 GB RAM, under the Windows XP Professional edition). Differences were quantified in terms of RMS errors ($\sqrt{bias^2 + variance}$), where bias is the mean difference and variance is the square root of the standard deviation of the differences. Student's t-test ($p < 0.05$) was used to determine if the RMS errors were significantly different from zero.

Experiment 3

The original full-length CT bone models were registered to 22 X-ray images for each knee as previously described. Synthetic X-ray images (Fig. 1b) were then created by ray tracing (Rhinoceros and Flamingo, Robert McNeel & Associates, Seattle, WA) the full-length CT bone models in these 3D poses. The same automated matching algorithm was then used to align

DOI 10.1002/jor

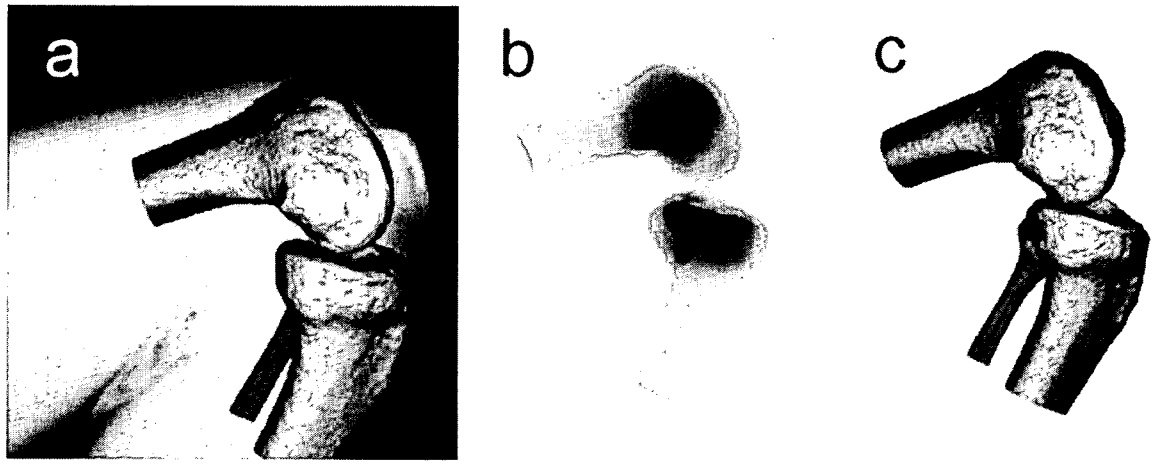

Figure 1. Matching of bone model to X-ray image (a), synthetic image generated using ray tracing (b), and matching of bone model to synthetic image (c).

shortened CT models and the MRI-derived bone models independently to the synthetic images (Fig. 1c).[1,6] RMS errors were used to compare results from the CT and MRI models. Paired t-tests ($p < 0.05$) were used to determine if there were significant differences.

RESULTS

Experiment 1

The differences between CT and MRI model surfaces (mean ± 1 SD) for the femur and tibia were -0.11 ± 0.81 mm and -0.14 ± 0.67 mm in subject 1, -0.23 ± 0.48 mm and -0.13 ± 0.48 mm in subject 2, and -0.12 ± 0.60 mm and -0.15 ± 0.77 mm in subject 3 (Fig. 2).

Experiment 2

Significant differences were found in three of six parameters (Table 1). RMS differences averaged 1.2 mm for sagittal plane translations, 2.3 mm for mediolateral translations, and 1.7° for all rotations.

Experiment 3

Average RMS errors for tibiofemoral poses were 0.74 mm for sagittal translations, 2.0 mm for mediolateral translations, and 1.4° for all rotations with MRI models. Average RMS errors were 0.53 mm for sagittal translations, 1.6 mm for mediolateral translation, and 0.54° for all rotations with the CT models (Table 2). The total amount of motion observed for each subject is shown in Table 3.

DISCUSSION

Single-plane X-ray imaging and model-based shape matching appear to provide kinematic measurements with sufficient certainty to assess

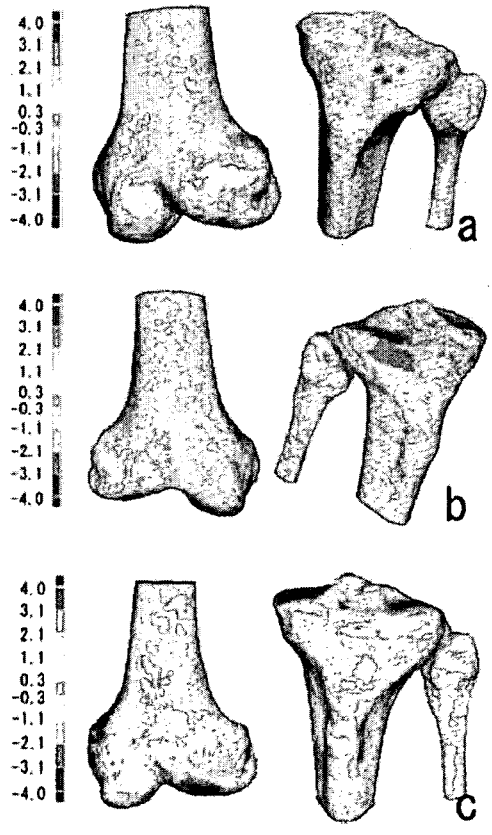

Figure 2. Three-dimensional distance measurement from CT model to MRI model (mm). (a) Subject 1, (b) subject 2, and (c) subject 3.

Table 1. Kinematic Differences When Using MRI– and CT–Derived Bone Models with In Vivo Images (RMS Differences)

Parameter	Subject 1	Subject 2	Subject 3	Average
Anterior–posterior translation (mm)	0.96	0.94	2.28	1.39
Superior–inferior translation (mm)	1.05	1.16	0.84	1.02
Medial–lateral translation (mm)	2.68	1.89	2.32	2.30*
Flexion–extension (°)	1.06	1.17	1.49	1.24*
Internal–external rotation (°)	2.35	0.92	1.54	1.60*
Varus–valgus (°)	1.82	3.42	1.71	2.32

*$p < 0.05$ from 0.

normal and pathological knee motions using either MRI– or CT–derived bone models. Nonetheless, measurement performance with CT–derived bone models was superior to measurements performed with MRI–derived models.

The results with CT–derived models improved significantly from our previous study, where only the exterior bone contours were used for shape matching.[6] Using only exterior contours resulted in average RMS errors of 1.8 mm for sagittal plane translations, 10.6 mm for mediolateral translations, and 1.1° for rotations, compared to 0.53 mm, 1.6 mm, and 0.54°, respectively, for rotations in the present study. Including internal edges for shape registration, specifically the occluded condyles of the femur and tibia and the head of the fibula, significantly improved shape-matching performance.[2] Kinematic measurement performance using single-plane fluoroscopic projections and CT–derived bone models was previously reported.[2] Komistek and colleagues reported measurement precision of 0.45 mm for sagittal plane translation and 0.66° for rotation, both comparable to our current study. Our results are also comparable to measurements using biplane radiographics and CT–derived bone models: RMS error of 0.23 mm for translations and 1.2° for rotation.[7] However, biplane techniques have more uniform errors, whereas single-plane techniques have much higher uncertainties for translations perpendicular to the image plane. No previous study exists to compare for the results with MRI–derived bone models.

Bony contours are less distinct in X-ray projections than the boundaries of metallic implants.[7] Fregly and colleagues showed that biased edge detection can be a primary factor limiting bone-model registration accuracy.[6] Thus, it is critical to adjust X-ray exposure parameters carefully to achieve good contrast around and within the joint. This is especially true for the tibia and fibula, where the fibular head tends to be obscured by the tibia and dense surrounding soft tissue, and the tibial condyles and tubercle are easily overpenetrated by the X-ray beam. Clearly defined, these bony features significantly reduce measurement uncertainty for tibial varus–valgus and internal–external rotation. Use of a high-resolution flat panel detector in the present study permitted adequate definition of these bone features. Image resolution also will affect shape-matching performance and measurement bias. Hardware and software limitations required the flat-panel detector images (1985 × 1490 pixels) to be resampled to 512 × 512 pixels for this analysis. Using higher resolution images, measurement bias could be decreased and measurement precision increased regardless of bone model source.

Table 2. Mean Kinematic Errors When Using MRI– and CT–Derived Bone Models with Synthetic Images (RMS Error)

	Subject 1		Subject 2		Subject 3		Overall		
Tibiofemoral Kinematics	MRI	CT	MRI	CT	MRI	CT	MRI	CT	*t*-Test
Anterior–posterior translation (mm)	0.60	0.44	0.84	0.56	1.19	0.97	0.88	0.66	0.024
Superior–inferior translation (mm)	0.68	0.40	0.46	0.35	0.64	0.44	0.59	0.40	0.057
Medial–lateral translation (mm)	1.54	1.96	2.69	1.34	1.69	1.47	1.97	1.59	0.54
Flexion–extension (°)	0.46	0.27	0.88	0.55	0.98	0.43	0.77	0.42	0.077
Internal–external rotation (°)	2.11	0.43	0.78	0.59	1.41	0.63	1.43	0.55	0.18
Varus–valgus (°)	2.28	0.61	1.34	0.64	1.93	0.67	1.85	0.64	0.049

DOI 10.1002/jor